european burn journal

MDPI

Article

Divulging the Complexities of Deep Partial- and Full-Thickness Burn Wounds Afflicted by *Staphylococcus Aureus* Biofilms in a Rat Burn Model

Alan J. Weaver, Jr., Kenneth S. Brandenburg, S. L. Rajasekhar Karna, Christopher Olverson and Kai P. Leung *

Combat Wound Care Research Team United States Army Institute of Surgical Research, JBSA Fort Sam Houston, San Antonio, TX 78234-7767, USA; alan.j.weaver3.ctr@mail.mil (A.J.W.J.); kenneth.s.brandenburg2.civ@mail.mil (K.S.B.); sailakshmirajasekh.karna.ctr@mail.mil (S.L.R.K.); christopher.olverson.mil@mail.mil (C.O.)

* Correspondence: kai.p.leung.civ@mail.mil

Abstract: Every year, thousands of soldiers and civilians succumb to burn wound trauma with highly unfavorable outcomes. We previously established a modified Walker-Mason rat scald model exhibiting a *P. aeruginosa* infection. Here we characterize deep partial- (DPT) and full-thickness (FT) burn wounds inoculated with *Staphylococcus aureus*. Male Sprague-Dawley rats (350–450 g) inflicted with 10% total body surface area burn inoculated with *S. aureus* ($10^{3–5}$ CFU/wound) were monitored over an 11-day period. *S. aureus* rapidly dominated the wound bed, with bacterial loads reaching at least 1×10^9 CFU/g tissue in all wounds. Within 3 days, *S. aureus* biofilm formation occurred based on genetic transcripts and Giemsa staining of the tissue. *S. aureus* infection resulted in a slightly faster recruitment of neutrophils in FT wounds, which was related to necrotic neutrophils. The extent of the inflammatory response in *S. aureus* infected burn wounds correlated with elevated G-CSF, GM-CSF, GRO/KC and/or TNF-α levels, but a majority of pro- and anti-inflammatory cytokines (IL-1β, IL-6, IFN-γ, IL-10, and IL-13) were found to be suppressed, compared to burn-only controls. *S. aureus* infection resulted in dynamic changes in DAMPs, including elevated HMGB-1 and reduced levels of circulating hyaluronan within FT wounds. *S. aureus* also reduced complement C3 at all time points in DPT and FT wounds. These changes in DAMPs are believed to be correlated with burn severity and *S. aureus* specific bioburden. Collectively, this model showcases the evasiveness of *S. aureus* through dampening the immune response to flourish in the burn wound.

Keywords: *Staphylococcus aureus*; DAMPs; burn wound; cytokine; infection; Rat Burn Model

Citation: Weaver, A.J., Jr.; Brandenburg, K.S.; Karna, S.L.R.; Olverson, C.; Leung, K.P. Divulging the Complexities of Deep Partial- and Full-Thickness Burn Wounds Afflicted by *Staphylococcus Aureus* Biofilms in a Rat Burn Model. *Eur. Burn J.* **2021**, *2*, 106–124. https://doi.org/10.3390/ebj2030009

Academic Editor: Naiem Moiemen

Received: 11 June 2021
Accepted: 27 July 2021
Published: 2 August 2021

1. Introduction

Burn injury is a traumatic event that breaches the barrier between the human's environment and the first line of defense—the skin. The moment this barrier is breached, the host is immediately put at a disadvantage as the burned skin becomes a nutrient-rich niche serving as a nidus for infection by the surrounding microflora of endogenous and exogenous origins [1–3]. Aside from the skin barrier being compromised, the host's immune system also enters a dysfunctional state, based on the area burned that is not amenable to healing or defense against pathogenic microorganisms. Soldiers are at particular risk as they are likely injured in austere environments that lack sterility and prevents the use of common burn injury treatments, such as topical wound rinse for wound cleansing and antimicrobial creams, which include Sulfamylon® and Silvadene®, for infection control [4–7]. However, it has been shown that, on average, regardless of the combat situation, soldiers typically face 10% total body surface area (TBSA), which are primarily located on their hands or face [6]. Similar trends of TBSA and burn location have been noted within the civilian world [8], where there are an estimated 180,000 deaths per year worldwide caused by fire [9]. Of those hospitalized, studies have identified infection as the root cause of death

for 42–65% of burn patients, which again stems from the immune-compromised state of the victim [10–13]. Overall, this speaks to the need for clear models of burn wounds that not only recapitulate the infective scenario, i.e., infections and diverse host responses elicited, but also provide avenues for testing novel therapeutics.

The severe damage to tissue and complex milieu of biomolecules within the burn wound offers an opportunistic environment for microbial infection. *Staphylococcus aureus* is a well-known opportunistic pathogen, which commonly causes skin and soft-tissue infections [14–16]. This Gram-positive bacterium resides in about 30% of the population and commonly causes both community- and hospital-acquired infections [17,18]. The immunocompromised state of burn patients puts them at serious risk for developing a *S. aureus* infection. Second to *Pseudomonas aeruginosa*, *S. aureus* is one of the most common pathogens known to infect burn victims, being among the first to colonize the wound following the trauma [1]. The seriousness of *S. aureus* infection is multifactorial, but includes its ability to form biofilms and evade the host immune system. Typically, *S. aureus* is recognized by Toll-like Receptors (TLRs) 2 and 9, which would ultimately trigger the NF-κB cascade to eliminate the invading organism [19,20]. However, encapsulation of individual bacterial cells by an extracellular matrix, as in *S. aureus* biofilms, provides protection from host recognition and phagocytosis of the pathogen. Furthermore, virulence factors released by *S. aureus* causes reduced opsonization and phagocytic activity, leading to impairment of macrophages and neutrophils [21–24]. This highlights the precarious state of the burn victim as they must not only contend with a dysfunctional immune system as it relates to the injury, but also with a bacterium that has evolved to evade that same impaired host defense system.

In our previous reports, we have established a modified-Walker Mason burn model for deep partial- and full-thickness injury, along with infection with *P. aeruginosa* [25–27]. These studies investigated the kinetics of *P. aeruginosa* biofilm formation, as well as the host-response to the burn injury under these infection conditions. In the present study, we utilized the burn model to investigate the infective nature of a clinical MRSA strain (TCH1516) to understand the kinetics of the Gram-positive pathogen and host response under these burn conditions. In this study, *S. aureus* readily formed biofilms within the burn eschar in both DPT and FT burn wounds based on transcriptional analysis, as well as several elicited virulence factors. Relative to the previous model with *P. aeruginosa*, the local inflammatory response and recruitment of cells induced by *S. aureus* in this study was not as extensive. However, *S. aureus* infection of DPT and FT burn wounds resulted in dynamic changes in key danger-associated molecular patterns (DAMPs) within the circulatory system. Additionally, compared to burn-only controls, a majority of pro- and anti-inflammatory cytokines (IL-1β, IL-6, IFN-γ, IL-10, and IL-13) were found to be suppressed in *S. aureus* infected burn wounds. Results of this investigation will be used in understanding more complex infections, involving multiple pathogens within the same wound bed. Furthermore, this study provides the foundational work for formulating novel therapeutic treatments of burn wound infections involving *S. aureus* to improve the current standard of care.

2. Materials and Methods

2.1. Bacterial Strain

The methicillin-resistant Staphylococcus aureus strain TCH1516 was purchased from the American Type Culture Collection (ATCC, Cat. No. BAA-1717). The MRSA strain TCH1516 is a clinical strain that was originally isolated at the Texas Children's Hospital in Houston, TX, USA. To prepare the bacteria for use in the model, cultures were grown overnight in Trypticase Soy Broth (TSB; Becton, Dickinson and Co., Sparks, MD, USA) and then sub-cultured the day of the burn to mid-log phase, prior to being diluted to desired concentrations for inoculation. Final infectious doses were 10^3, 10^4, and 10^5 CFU per wound.

2.2. Overview of Scald Burn Model

Due to the complexity of the study, three identical experiments were performed for each type of burn. Per IACUC requirements, each experiment consisted of two animals per infectious group, per post-operative day (POD), as well as one control animal per POD. This led to a total of n = 6 per infectious group, per POD, and n = 3 for control per POD. The nature of the scald burn wound model is described below.

A deep partial-thickness (DPT) or full-thickness (FT) scald burn was inflicted on the dorsum of an anesthetized rat by methods previously described [25,26]. In brief, the day preceding the burn, male Sprague-Dawley rats weighing 350–450 g were anesthetized using isoflurane (Forane) in order to shave and depilate the dorsum. A subcutaneous injection of Buprenorphine SR LAB (1.2 mg/kg, Zoopharm Pharmacy, Windsor, CO, USA) for pain management was also given.

On the day of the burn, a 10% total body surface area (TBSA, based on Meeh's formula [28]) DPT or FT burn was administered to anesthetized rats by subjecting the rat's dorsum to near-boiling (99 °C) water for 3 s (DPT burn) or 6 s (FT burn). Immediately following the burn, an epicutaneous inoculation of 100 µL phosphate buffered saline (PBS) containing 10^3, 10^4, or 10^5 CFUs of *S. aureus* (strain TCH1516) or PBS only for control animals was applied to the wound. Once inoculated, a non-adherent interface dressing was applied to the wound, along with a Tegaderm™ Film (3 M Health Care, St. Paul, MN, USA), which was secured to the perimeter using NOTAPE silicone adhesive (Vapon, Inc. Fairfiled, NJ, USA). Lastly, rats were placed in a previously designed jacket to prevent wound tampering, and monitored over an 11-day period.

Euthanization was performed on PODs 1, 3, 7, and 11, for burn wound assessment of injury and infection, as well as wound collection. At each endpoint, animals were anethesized with 100 mg/kg Ketamine HCl (Zetamine, MWI Veterniary Supply Co. Boise, ID, USA) and 10 mg/kg Xylazine (Akorn Animal Health, Inc., Lake Forest, IL, USA). Blood was acquired via cardiac puncture, followed immediately by euthanization by intra-cardiac injection of Fatal-Plus® (Vortech Pharmaceuticals, Ltd., Dearborn, MI, USA). Euthanasia was confirmed by lack of cardiac movement, pulse, and breathing as specified by the AVMA Guidelines for the Euthanasia of Animals: 2013 Edition [29]. Once euthanasia was confirmed, the burn wound was excised and processed for bioburden, pathology, and biochemical analyses.

2.3. Bioburden Quantification

To establish bioburden, isolated tissue was placed in pre-weighed bead lysis tubes, weighed to determine the tissue weight, and homogenized in PBS with a FastPrep®-24 Tissue Homogenizer (MP Biomedicals, LLC, Santa Ana, CA, USA). Samples were serially diluted with PBS prior to plating on Trypticase soy agar containing 5% sheep's blood (#221261, Becton, Dickinson and Co., Franklin Lakes, NJ, USA), as well as *S. aureus* isolation agar (#214982, Becton, Dickinson and Co.), using a WASP 2 Spiral Plater (Microbiology International, Frederick, MD, USA). Viable CFUs were enumerated using a ProtoCOL 3 Colony Counter (Microbiology International). Quantification results were based on n = 3 per POD for controls and n = 6 per group per POD for infections.

2.4. Gene Transcript Analysis

Expression levels of several genes associated with *S. aureus* biofilms (ureB, ureC, arcC, acrR, sasF, sdrC, arcB (argF), and icaR) and virulence (hla, luks-PV, and splF) were quantified, along with four distinct housekeeping genes (gmk, gyrA, and femA), using a QuantiGene Plex Assay (Assay ID M18061403, Affymetrix, Inc. Santa Clara, CA, USA) following the manufacturer's procedure for Frozen Tissue Homogenates, as previously described [26]. Briefly, samples were initially pulverized under liquid nitrogen and then lysed for 15 min at 37 °C with lysis mixture (cold TES Buffer with Lysozyme and Lysostaphin), followed by 15 min incubation at 65 °C with Proteinase K Homogenization solution. Samples were centrifuged for 5 min at 4000 rpm to isolate supernatants, which were stored −80 °C

until analysis. To perform analysis, homogenates were initially thawed and incubated at 37 °C for 30 min and then incubated with the Working Bead Mix, containing Proteinase K and the Capture Beads, in a hybridization plate at 54 °C for 18 h with gentle shaking at 600 rpm. Following incubation, the sample was transferred to the Magnetic Separation Plate and subjected to 3 washes with Wash Buffer in between 1 h incubations at 50 °C with Pre-Amplifier Solution, Amplifier Solution, and Label Probe Solution. Following addition of the Label Probe Solution, samples were incubated with SAPE Working Reagent for 30 min at room temperature and washed 3× with SAPE Wash Buffer. Prior to analysis, samples were mixed with 130 µL of SAPE Wash Buffer, shaken for 3 min at 800 rpm, and immediately read on a Bio-Plex 200 System with Bio-Plex ManagerTM Software Version 6.1 Build 727 (BioRAD Laboratories, Inc. Hercules, CA, USA). For planktonic controls, 2 mL of the mid-log phase cell culture used to inoculate the burn wounds was pelleted. The pellet was treated with 2 mL of RNAprotect (Qiagen, Hilden, Germany, Cat. No. 76506) and stored at −80 °C until further processing. The pellet was processed in the same manner as the tissue, but without liquid nitrogen pulverization. All transcript analysis was the result of n = 3 per POD for controls and n = 6 per group per POD for infections.

2.5. Histopathological Assessment

Following excision, cross-sections of the tissue were immediately fixed in 10% buffered formalin in PBS (Fisher Scientific, Kalamazoo, MI, USA) for at least 48 h. Tissue was processed for routine embedding in paraffin wax, followed by sectioning (4–5 µm). Slides were stained with hematoxylin-eosin (H&E) and submitted for pathological assessment by a trained pathologist. Pathological scores, based on total inflammatory cell infiltration for overall inflammation, were scaled as follows: 0—none, 1—minimal, 2—mild, 3—moderate, or 4—marked. Scoring for individual cell infiltration was defined as follows: zero is none, one is 0–10%, two is 10–25%, three is 35–50%, and four is >50%. A second set of H&E slides were also stained with Giemsa for visualization of the microflora. Results from pathological assessment and microflora visualization were based on n = 3 per POD for controls and n = 6 per group per POD for infections.

2.6. Blood Collection and Processing

Serum separator (Vacuette® 454228P, Greiner Bio-One, Kremsmünster, Austria) tubes were used for blood collection via cardiac puncture. All serum was isolated per manufacturer's instructions and stored at −80 °C until evaluated.

2.7. Local Cytokine & Chemokine Panel

Local cytokines/chemokines were assessed as previously described [27]. In brief, 7 mm biopsy punches from the wound bead were pulverized under liquid nitrogen, followed by homogenization in lysis buffer (Bio-Plex® Cell Lysis Kit, #171304011, Bio-Rad, Hercules, CA, USA). Following a freeze-thaw cycle, homogenates were sonicated 5 s and centrifuged to collect supernatants. Protein content was established using a Pierce™ BCA Protein Assay Kit (#23227, Thermo Fisher Scientific, Waltham, MA, USA). All samples were normalized to 900 µg/mL protein and then assayed using a Bio-Plex Pro™ Rat Cytokine 23-Plex (#12005641, Bio-Rad, Hercules, CA, USA) kit, which was analyzed on a Bio-Plex™ 200 System (Bio-Rad, Hercules, CA, USA) and quantified using the BioPlex Manager 6.1 software. Cytokine and chemokine analysis was based on n = 3 per POD for controls and n = 6 per group per POD for infections.

2.8. Danger Associated Molecular Patterns Analysis

2.8.1. Myeloperoxidase Activity

Myeloperoxidase (MPO) activity was assayed from a 7 mm biopsy punch collected from the wound bed using a Fluoro MPO Myeloperoxidase Detection Kit (Cell Technology, Inc., Mountain View, CA, USA), as previously described [25]. In brief, one 7 mm biopsy punch was pulverized under liquid nitrogen using a Bessman Tissue Pulverizer (Spectrum,

Inc., Rancho Dominguez, CA, USA), homogenized with an IKA T10 basic Ultra Turrax tissue homogenizer (IKA Works, Inc., Wilmington, NC, USA), and then centrifuged at 12,000× *g* for 20 min at 4 °C. Pellets were re-suspended in MPO solubilization buffer, homogenized again, and then sonicated for 5 s with a Sonic Dismembrator Model 100 (Fisher Scientific, Kalamazoo, MI, USA). Samples were subjected to two freeze-thaw cycles and then centrifuged to isolate supernatants, which were stored at −80 °C until needed. Protein concentrations in supernatants were quantified using a Pierce™ BCA Protein Assay Kit (#23227, Thermo Fisher Scientific, Waltham, MA, USA). For MPO quantification, samples were normalized to 350 µg/mL protein and then assayed per the manufacturer's instructions for detection of MPO. MPO analysis was based on n = 3 per POD for controls and n = 6 per group per POD for infections.

2.8.2. High Mobility Group Box-1

High mobility group box-1 (HMGB-1) protein present in the serum was quantified using a Rat HMGB-1 ELISA kit (#50155150, Fischer HealthCare, Inc., Waltham, MA, USA). Samples were diluted as needed with provided diluent prior to being assayed on a DSX® Automated ELISA System (Dynex Technologies, Inc., Chantilly, VA, USA) per kit manufacturer's instructions. HMGB-1 analysis was based on n = 3 per POD for controls and n = 6 per group per POD for all infections, except for DPT 10^3 inoculum on PODs 3 and 11 (n = 5).

2.8.3. Hyaluronan

For hyaluronan analysis, serum was diluted 1:4 with provided diluent prior to being assayed with a Hyaluronan Quantikine ELISA Kit (DHYLA0, R&D Systems Inc., Minneapolis, MN, USA). Assays were performed on a DSX® Automated ELISA System per kits manufacturer's instructions. Hyaluronan analysis was based on n = 3 per POD for controls and n = 6 per group per POD for all infections, except for the following: DPT 10^3 inoculum on POD 3 (n = 5) and POD 11 (n = 4); DPT 10^4 inoculum on POD 7 (n = 4); and FT 10^5 inoculum on POD 3 (n = 5).

2.8.4. Complement C3

Complement C3 present in the serum was quantified using a Rat Complement C3 ELISA kit (ab157731, Abcam, Cambridge, MA, USA). Samples were diluted 1:10,000 using provided diluent and then assayed using the DSX® Automated ELISA System per the manufacturer's instructions. Complement C3 analysis was based on n = 3 per POD for controls and n = 6 per group per POD for all infections, except for the following: DPT 10^3 inoculum on POD 3 (n = 5) and POD 11 (n = 4); and DPT 10^4 inoculum on POD 7 (n = 4).

2.9. Statistical Analysis

All statistical analysis was performed in GraphPad Prism 8 (GraphPad Software, San Diego, CA). Unless otherwise noted, values represent the mean value with standard deviations with significant differences based on 2-way ANOVA analysis with a Šidák post-hoc test.

3. Results

3.1. Bacterial Burden and Biofilm Formation

In the case of both DPT and FT burn injury, bacterial burden (*S. aureus* or total bacteria) within the tissue increased over the 11-day period. *S. aureus* selective plates confirmed no contamination of the pathogen in burn-only control groups (Figure 1A). The total bioburden within the FT burn-only controls increased more steadily and consistently compared to DPT burn-only; however, the DPT controls had a slightly elevated bioburden by POD 11 (Figure 1B). In infected groups, *S. aureus* was the most predominant species composing the bioburden in DPT and FT burn wounds. However, compared to 10^3 and 10^4 (Figure S1), only the 10^5 CFU inoculum of *S. aureus* provided consistency in infection rates, with CFUs

plateauing at by POD 3 for both DPT and FT burns. With the 10^5 inoculum, levels of *S. aureus* were significantly higher in DPT burn wounds at PODs 7 and 11 compared to FT burn wounds. Similar trends were seen for the 10^3 and 10^4 CFU inoculums; however, the amount *S. aureus* present was variable, particularly at early time points for both DPT and FT burn wounds (Figure S1).

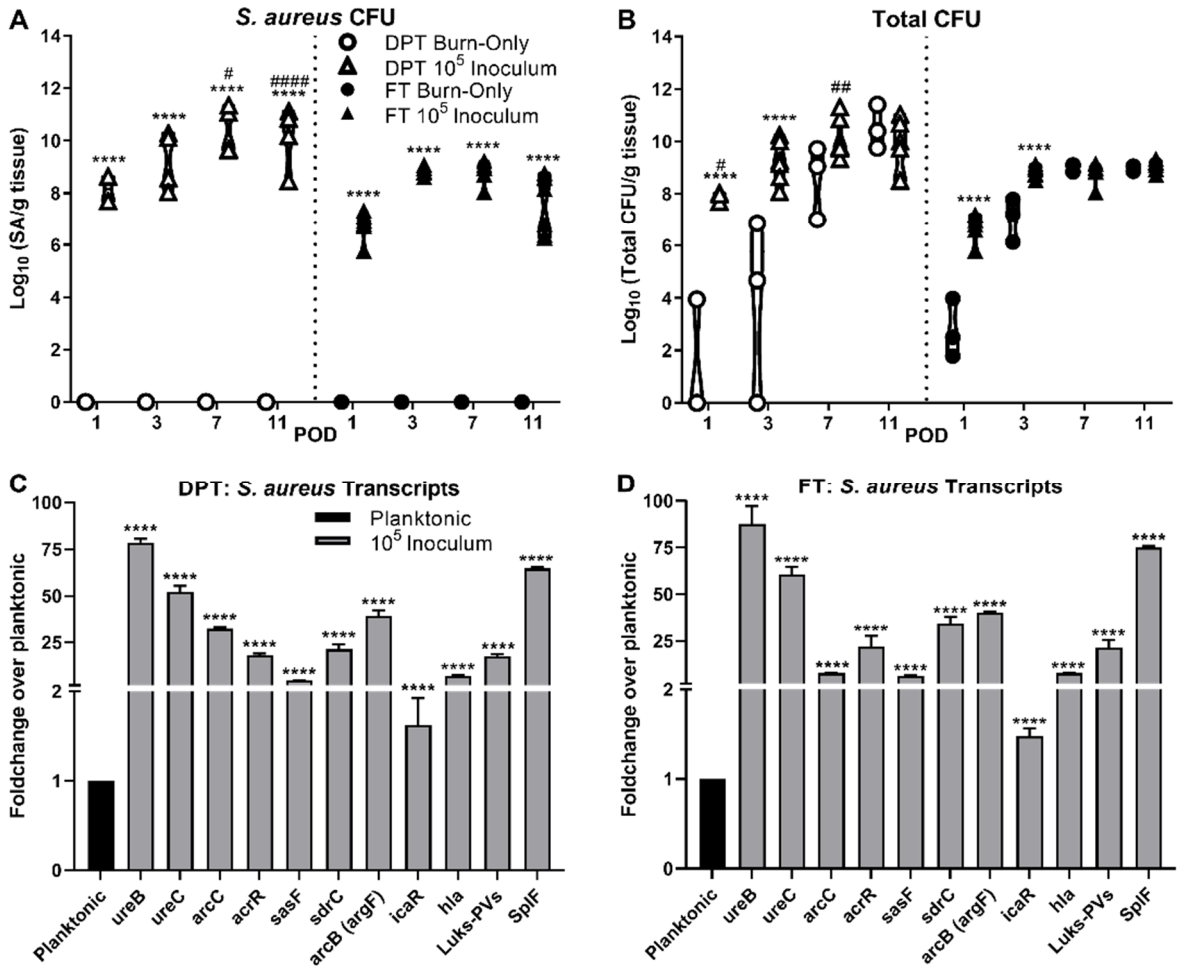

Figure 1. Bioburden and gene transcriptional analysis within DPT and FT Burn Wounds. *S. aureus* dominates the wound bed for both DPT and FT burn wounds relative to the total bioburden, based on viable CFU counts (**A** and **B**, **** $p < 0.0001$, compared to burn-only). Despite the lack of inoculation with *S. aureus,* there is still a clear increase in bioburden from the native flora (**B**). DPT burn wounds had significantly more *S. aureus* present at PODs 7 and 11, compared to FT infected burn wounds; as well as overall bioburden at PODs 1 and 7 ($^{\#}$ $p < 0.05$, $^{\#\#}$ $p < 0.01$, $^{\#\#\#\#}$ $p < 0.0001$). Transcriptional analysis of genes related to biofilm processes of *S. aureus* were upregulated in both DPT (**C**) and FT (**D**) burn wounds at POD 3, with the exception of icaR, which is a suppressor of the ica genes. Transcriptional values are represented as the average fold-change over planktonic cells ± standard deviation. Transcriptional differences were based on normalized values of planktonic and burn wound isolated cells (**** $p < 0.0001$).

In order to establish biofilm formation within each burn wound scenario, several genetic markers that are relevant to biofilm formation and/or virulence in *S. aureus* were evaluated over the course of the infection (Figure 1C,D and Figure S2). By POD 3, the 10^5 inoculum showed significant increases in all biofilm related markers, with most at or above a 2-fold increase, relative to planktonic expression (Figure 1C,D). These included genes related to anaerobic metabolism (ureB/C, acrR, arcC) and adhesion/attachment (sdrC and sasF). Of the genes assayed, icaR was the only gene found to have less than 2-fold change at POD 3. Virulence related genes hla, Luks-PV, and splF were also noted to be elevated at this point in infection. These trends in *S. aureus* biofilm gene expression

were also seen in the 10^3 and 10^4 inoculums, but with more variability in FT burn wounds relative to DPT wounds (Figure S2). Furthermore, several of the genes assayed were significantly increased in the 10^5 inoculum as early as POD 1 in both DPT and FT burn wounds (Figure S2). All genes maintained expression levels throughout the time course of infection.

Staining of the tissue with H&E plus Giemsa further confirmed bacterial presence within the tissue (Figure 2). Those wounds infected with *S. aureus* showed a heavy burden of cocci present in dense clusters throughout the tissue for both DPT and FT burn wounds at POD 3, with DPT burn wounds having slightly denser clusters than FT burn wounds. While cocci were also present in the burn-only controls, they were noted to be in smaller and sparser clusters located closer to the epithelial surface of the wound.

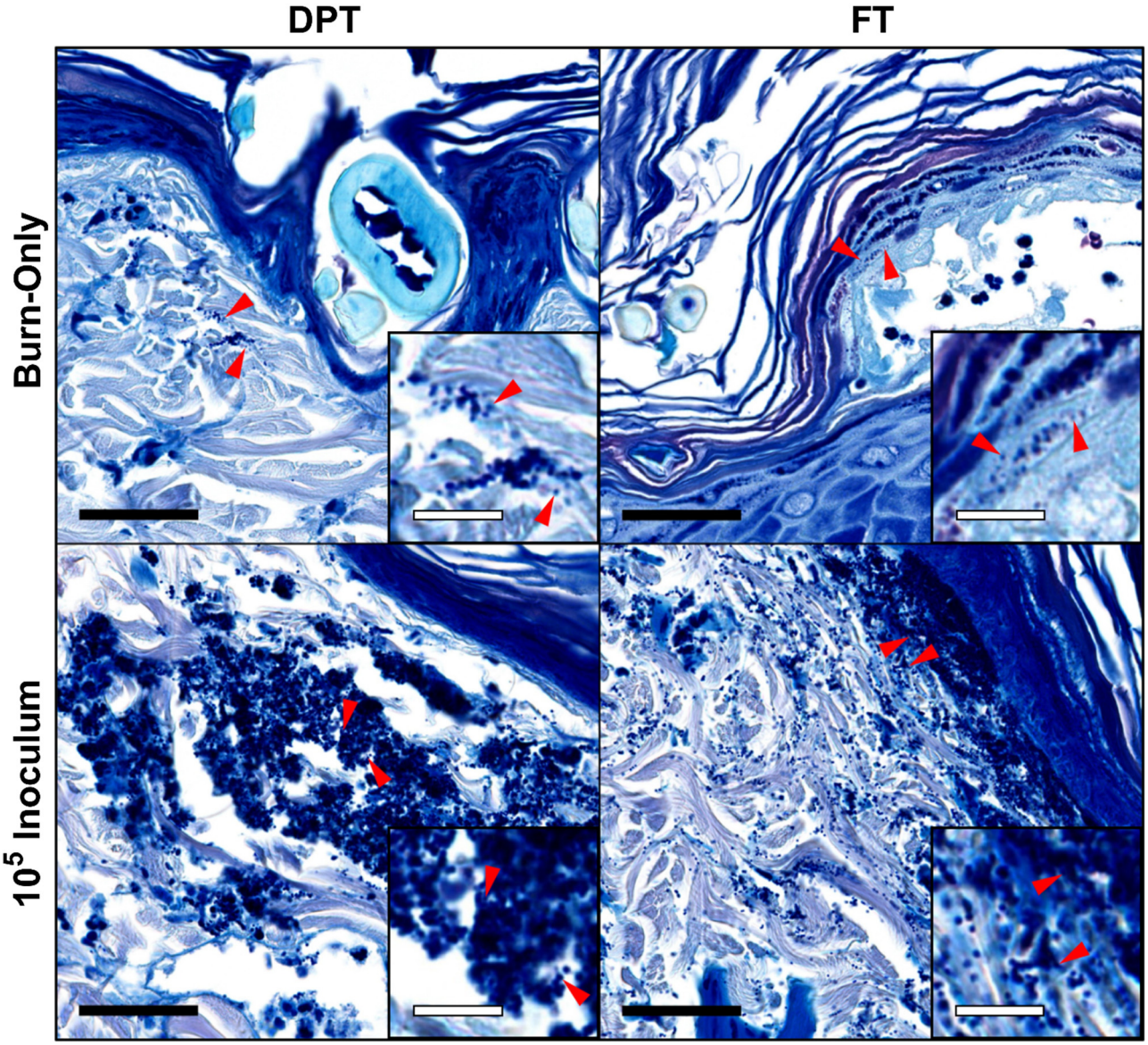

Figure 2. Visualization of *S. aureus* in DPT and FT burn wound tissue by H&E plus Giemsa staining of tissue. Burn-only wounds showed signs of colonization by cocci that are sporadic and showed minimal clustering. *S. aureus* infected wounds showed very dense clusters of cocci in 10^5 CFU inoculums in both DPT and FT burn wounds that reflect a more biofilm state of the bacteria. Red arrows indicate cocci and correlate with magnified insets. Black and white scale bars represent 40 μm and 10 μm, respectively. Magnifications of main images and insets are 63× and 189×, respectively.

3.2. Pathological Assessment & MPO Activity

Pathological assessment of H&E stained tissue showed overall inflammation for FT burn wounds (inoculated and non-inoculated) to trend higher than DPT burn wounds (Figure 3A); however, changes were not significant. DPT burn wound showed minimal changes in cellular recruitment, with the exception of a slightly higher trend of healthy neutrophils at POD 7 in all three infectious groups (Figure 3C and Figure S3C); but changes were not significant. Although similar levels of inflammation were reached by POD 11 between the 10^5 inoculum and burn-only wounds within each burn scenario, FT burn wounds exhibited slightly heightened inflammation at POD 3 when inoculated with *S. aureus*, but not significant. *S. aureus* had minimal to no effect on macrophages (Figure 3B) and healthy neutrophil (Figure 3C) recruitment in inoculated FT burn wounds, compared to controls. However, a slightly elevated trend in necrotic neutrophils was seen at POD 3 in FT burn wounds inoculated with 10^5 CFUs compared to burn-only samples at POD 3 (Figure 3D). The same trend was seen with the 10^4 inoculum. These mild changes in necrotic neutrophil with *S. aureus* infection of FT burns may be related to the earlier signs of overall inflammation and slightly elevated levels of MPO at POD 7 for all inoculums, albeit not significant (Figure S3E).

3.3. Local Cytokines

A dynamic cytokine and chemokine response was seen with respect to *S. aureus* infection at 10^5 inoculum within both burn wound scenarios. Significant increases in granulocyte (G-) and granulocyte macrophage colony stimulating factors (GM-CSF) were seen in DPT and/or FT burn wounds, while macrophage colony stimulating factory (M-CSF) was suppressed, relative to burn-only (Figure 4A–C). Among pro-inflammatory markers, only human-growth regulated onco-gene/keratinocyte chemoattractant (GRO/KC, i.e., CXCL-1, an IL-8 related chemokine) and tumor necrosis factor-alpha (TNF-α) were elevated in both DPT and FT burn infections compared to burn-only (Figure 4D,E). All others, including IL-1β, IL-6, IL-12p70, and IFN-γ, were significantly suppressed at times by *S. aureus* infection (Figure 4F–I). Significant suppression of the anti-inflammatory IL-10 was seen in FT infected burn wounds (Figure 4J), while IL-13 was suppressed at times in both DPT and FT infected burn wounds, relative to burn-only (Figure 4K). Similar trends and significance were also seen with 10^3 and 10^4 inoculums (Figure S4).

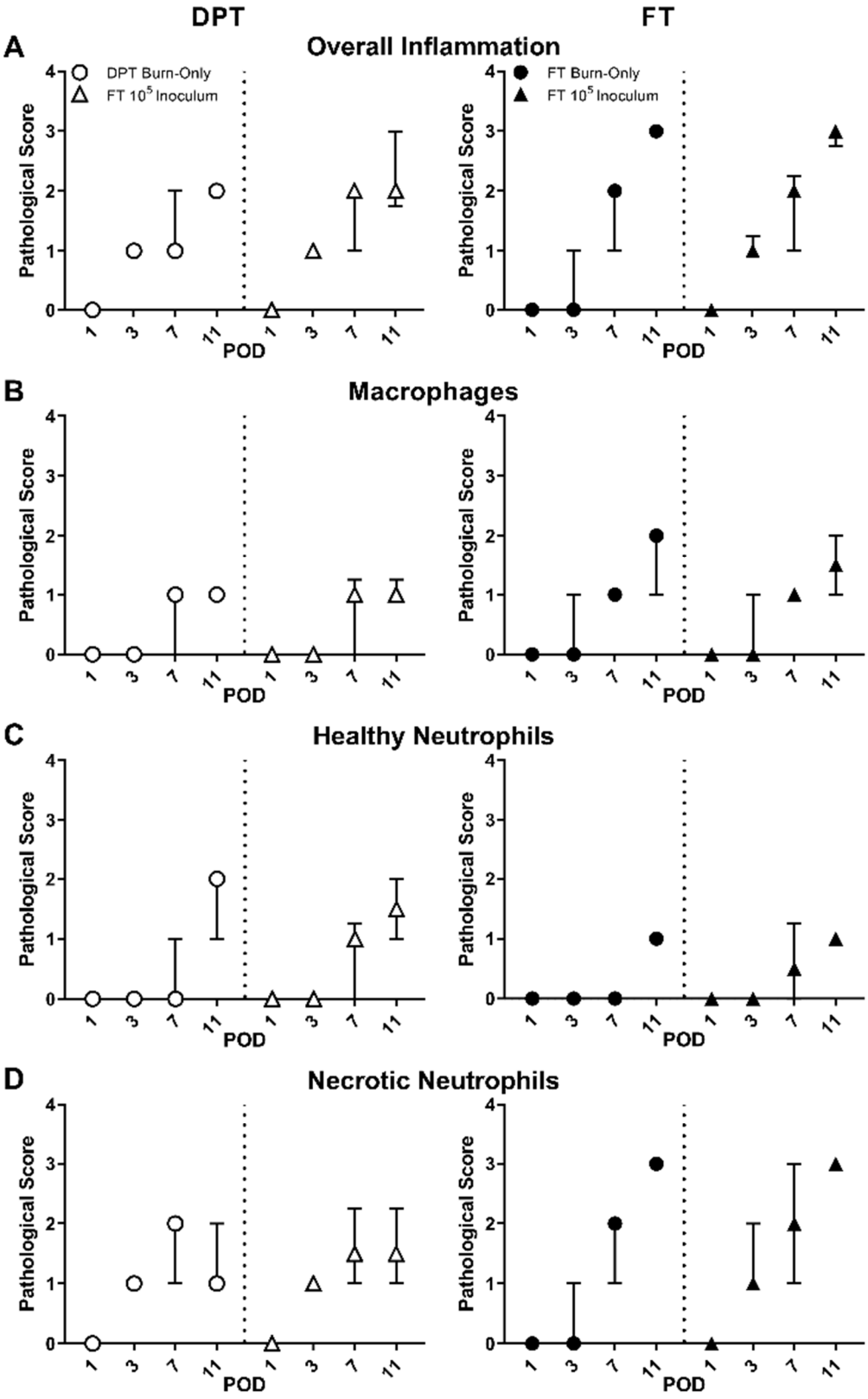

Figure 3. Pathological assessment of DPT and FT burn wounds. Pathological assessment revealed overall greater inflammation in FT burn wounds, with or without *S. aureus* infection (**A**). Macrophages remained unaffected by *S. aureus* infection (**B**). Healthy neutrophils trended slightly higher at POD 7 in DPT burn wounds infected with *S. aureus*, while necrotic neutrophils trended slightly higher in FT burn wounds (**C**). *S. aureus* also appeared to result in a slightly faster generation of necrotic neutrophils in FT burn wounds at POD 3 (**D**). Pathological scores are represented as the median with interquartile ranges.

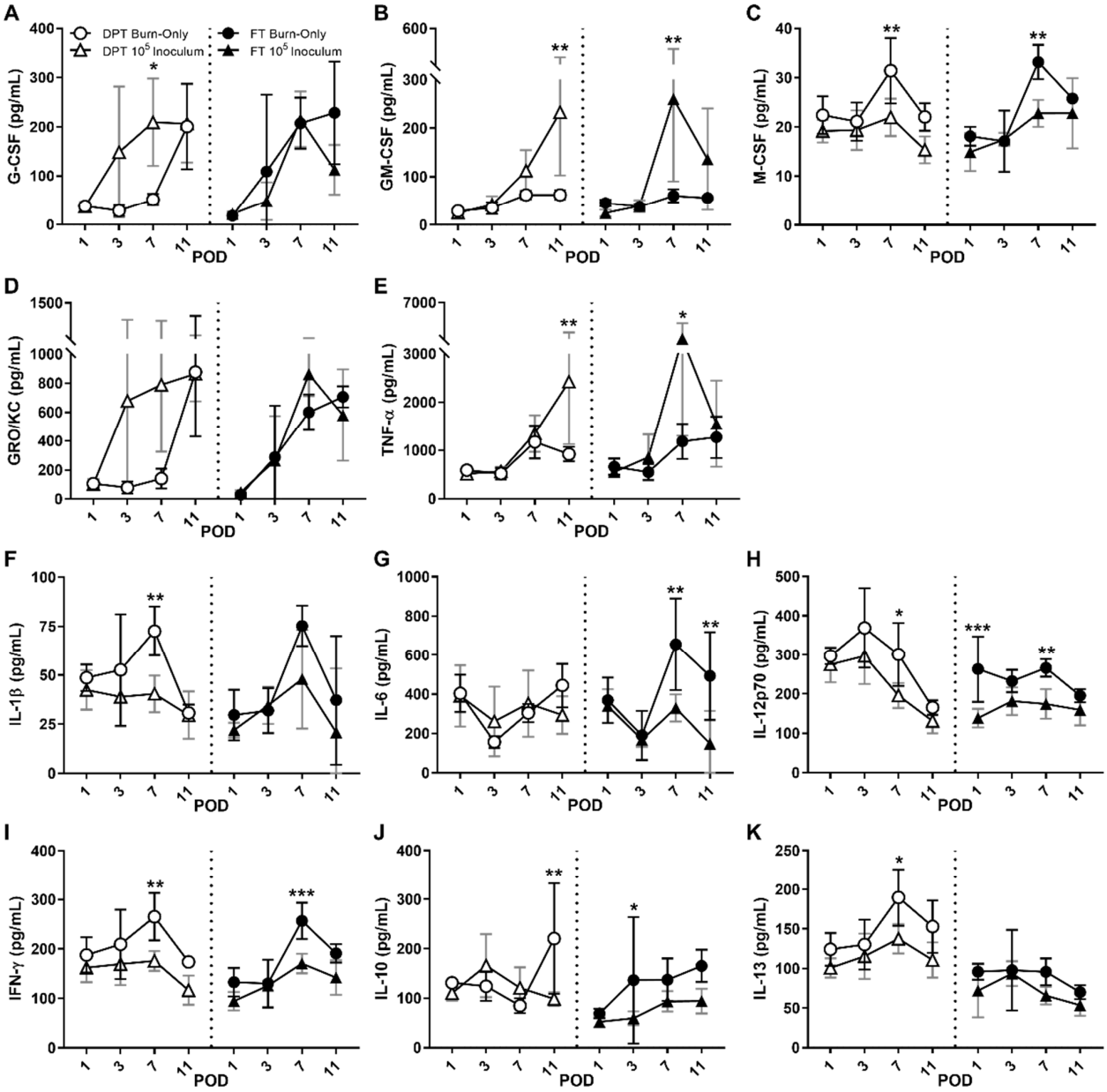

Figure 4. Local cytokine and chemokine responses within burn wounds following infection with *S. aureus*. Following infection with *S. aureus*, G-CSF (**A**) and/or GM-CSF (**B**) are elevated in DPT and FT burn wounds, while M-CSF (**C**) is suppressed, which may play a role in overall neutrophil and macrophages responses. Among pro-inflammatory cytokines, only GRO/KC (**D**) and TNF-α (**E**) are induced, while the majority show signs of suppression, including IL-1β (**F**), IL-6 (**G**), IL-12p70 (**H**) and IFN-γ (**I**). Anti-inflammatories IL-10 (**J**) and IL-13 (**K**) were suppressed in DPT and/or FT. Significant differences are denoted as either * $p < 0.05$, ** $p < 0.01$, or *** $p < 0.001$. Black and gray bars represent the standard deviation of burn-only and 10^5 inoculum, respectively.

3.4. DAMPS

HMGB-1 (Figure 5A) and HYL (Figure 5B) showed minimal changes in DPT burn wounds regardless of infection; however, complement C3 was significantly reduced in DPT and trended low in FT burn wounds in the presence of *S. aureus*, relative to burn-only controls (Figure 5C). FT burn inoculated with *S. aureus* also exhibited elevated levels of HMGB-1 at all time points compared to burn-only. HYL was reduced in S. aureus infected FT burn wounds, being significantly lower at POD 3. These effects on HMGB-1 and HYL

induced by S. aureus infection in FT burns were also seen in the 10^3 and 10^4 inoculums (Figure S5A,B). These *S. aureus* inoculum-dependent changes were also seen to govern the suppression of complement C3, which occurred at almost all time points for both DPT and FT burns for 10^4 and 10^5 inoculums (Figure 5C and Figure S5C).

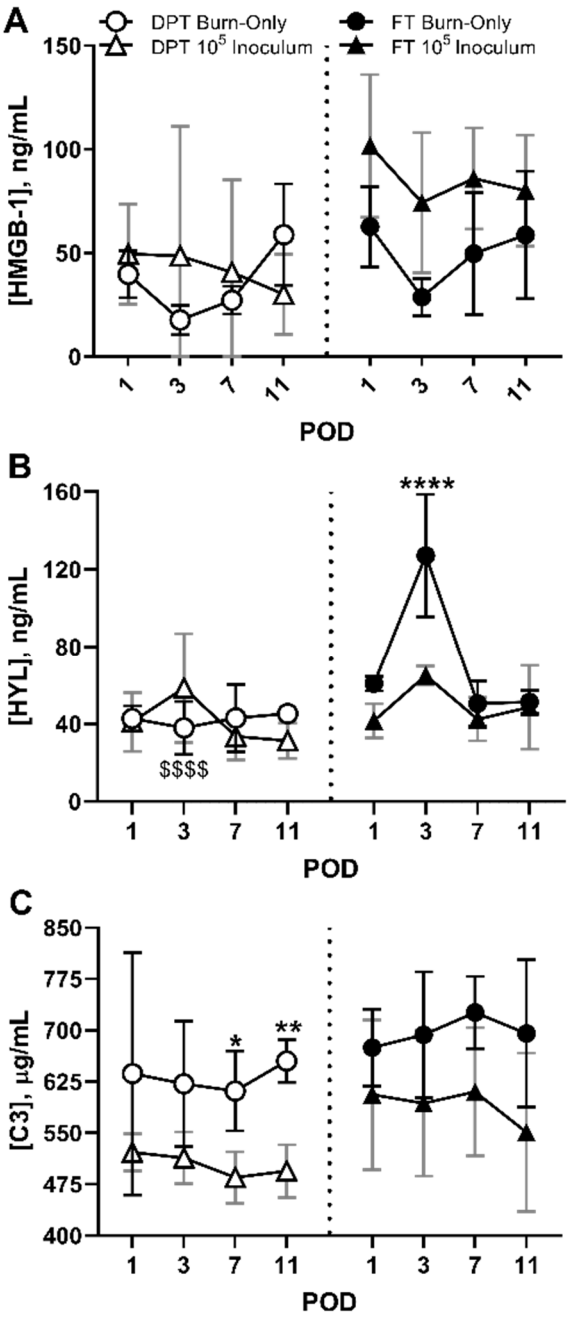

Figure 5. Systemic changes in DAMPs as a result of *S. aureus* infection within DPT and FT burn wounds. *S. aureus* induced minimal changes in HMGB-1 within FT burns (**A**), while also causing significant suppression of HYL (**** $p < 0.01$) that corresponds with the timing of biofilm formation at POD 3 (**B**). Although DPT burn wounds saw no differences in HYL or HMGB-1, HYL suppression correlated with the extent of injury as DPT burn-only controls had significantly less amounts of HYL at POD 3, relative to FT burn-only controls at POD 3 ($^{\$\$\$\$}$ $p < 0.001$). Relative to burn-only, a significant reduction in Complement C3 was seen in DPT burns infected with *S. aureus*, at PODs 7 and 11. A similar trend was seen in FT burn wounds infected with *S. aureus* (**C**), albeit not significant. Black and gray bars represent the standard deviations of burn-only and 10^5 inoculum, respectively (* $p < 0.05$, ** $p < 0.01$).

4. Discussion

Burn wound trauma causes a disruption of the primary barrier that protects humans from their surrounding environment, which places the victim in a vulnerable state. The injury alone generates a dynamic and un-orchestrated set of wound repair signals, which ultimately results in a poorly healed wound. Unfortunately, the factors governing this type of trauma are numerous, causing conflicting opinions on what is best for a given patient based on research and clinical investigations. The investigations undertaken here looked to build upon and re-evaluate our previous burn model of *P. aeruginosa* infection, by focusing on the host response to Gram-positive bacterium, *S. aureus* in burn wounds.

S. aureus exposure following DPT and FT burn injury resulted in rapid biofilm formation within the wound bed. While total numbers of viable bacteria at POD 1 were directly correlated with *S. aureus* inoculum levels, by POD 7 and 11 for FT and DPT burn wounds, respectively, all groups have gained similar bioburden levels regardless of the starting inoculum size. The results are largely consistent with growth kinetics seen in *P. aeruginosa* in the rat burn wounds previously established [25,26]. In contrast to our previous reports on *P. aeruginosa*, it was noted that *S. aureus* appeared to thrive better in the DPT burn wounds, having significantly more viable CFUs at PODs 7 and 11, relative to FT burn wounds infected with *S. aureus*. This elevation in CFUs in DPT versus FT burn wounds coincided with heavier clustering in cocci at POD 3 in DPT burn wounds infected with *S. aureus*, compared to FT burn wounds infected with *S. aureus*. It is unclear as to why *S. aureus* is able to thrive more in DPT burn wounds, but we speculate that it could be related in part to ease of nutrient access from devitalized tissue and/or the overall trend of less inflammation seen in DPT burn wounds, compared to FT burn wounds. It was noted that 10^3 and 10^4 inoculums of *S. aureus* showed some inconsistencies in growth at PODs 1 and 3, as well as lower expression levels of biofilm genes in FT burn wounds at POD 3. While this suggests that a 10^5 inoculum may be required for consistent infection in future studies involving this model, it is still notable that domination of the wound bed by *S. aureus* can occur with as little as 1000 CFUs.

While it appears that *S. aureus* dominates the wound bed ecosystem in both burn scenarios, it is important to note that non-inoculated control wounds showed equal numbers of resident bacteria in both scenarios, most likely derived from the environmental and residential skin microbiota that survived the burn trauma. This is consistent with our previous findings in burn controls, which raises the important point that wounds will remain colonized by the host's surviving natural skin microflora and/or those from the environment [30,31]. A previous study by our group on the microbiota of DPT burn wounds, absent of an inoculated pathogen, revealed that the inter-subject heterogeneity of the rat skin microbiota decreased as the burn wound progressed, while the relative abundance of wound resident *Staphylococcus* species (e.g., *S. sciuri* and *S. aureus*) increased by 50% compared to healthy skin [30,31]. While the natural microbiota are generally considered part of our healthy biome and beneficial, the bacterial shift that occurs following injury can cause some of these opportunistic species (e.g., Staphylococcus) to become pathogenic due to perturbations of the microbiome and a compromised host immune system as the results of thermal injuries. Of equal importance is that an inoculation with *S. aureus* results in a wound bed dominated by this Gram-positive pathogen, which highlights the opportunistic nature of this pathogen, and the need for awareness of the importance of other resident microbes, as a healthy skin resident microbe to resist colonization by opportunists.

Further support of biofilm formation within this model was provided based on expression pivotal biofilm related genes. Genes associated with adhesion and attachment, such as *sdrC* and *SasF*, as well as genes related to anaerobic metabolism (*ureB/C*, *acrR*, arcC) were all elevated by POD 3 [32–35]. Furthermore, minimal changes in *icaR*, a repressor of the *ica* gene family, suggests increased expression of polysaccharide intercellular antigen (PIA), which also plays a role in anaerobic biofilm formation [36]. Several virulence genes associated with biofilm formation, including *LukS-PV,* α-hemolyisin (*hla*), and *SplF* were also upregulated [37,38]. *LukS-PV* and *hla* have been shown to generate pores in several

immune cells, including neutrophils, macrophages, and leukocytes, which results in poor phagocytosis and cellular death [39,40]. *LukS-PV* in particular has been noted to induce NETosis, which leads to neutrophil cell death [41]. Furthermore, *SplF* expression leads to generation of serine proteases and is believed to be involved in infection of the host [42]. Collectively, these results suggest successful establishment of *S. aureus* biofilms within DPT and FT burn wounds at all test inoculums, providing a clinically relevant state of infection.

Aside from establishing the course of infection from a bacterial standpoint, we also investigated how the host responds to the *S. aureus* biofilm from a local and systemic standpoint. While our previous report with *P. aeruginosa* infection showed a high pro-inflammatory response with increased neutrophil infiltration, the case with *S. aureus* was not the same. Overall, inflammation trended greater in FT burn wounds with dense necrotic neutrophils compared to DPT burn wounds, but pathological assessment revealed that *S. aureus* infection caused minimal changes within each burn scenario. In FT burn wounds, inflammation was slightly increased at POD 3 in the 10^5 inoculum, which may be attributed to a slight increase in necrotic neutrophils compared to controls. This slight change may be related to the significant increases in expression of *hla* and *LukS-PV* in these biofilm-infected wounds, as well as slight elevations of MPO in all FT infected groups at POD 7. Although changes in neutrophil recruitment in the DPT and FT burn wounds infected by *S. aureus* were not significant, they were supported by significantly increased levels of several local cytokines/chemokines known for attracting or stimulating neutrophils, including G-/GM-CSF, GRO/KC, and/or TNF-α [43–45]. Furthermore, the lack of change in macrophage recruitment may be related to significant reductions in M-CSF and IL-6 in both DPT and FT infected wounds, which would disrupt their ability to clear the bacterial infection [46,47]. Overall, these changes may be related to a lack of recognition of the bacteria following biofilm formation that is established at POD 3, which alludes to the evasive nature of *S. aureus*.

Biofilm formation can serve as a defense mechanism for several microorganisms, including *S. aureus*. The matrix that surrounds the bacteria under these biofilm conditions not only results in reduced penetration of antimicrobials, but can also block recognition of the bacteria by the host's immune system and prevent an appropriate immune response [48–50]. Attenuation of the immune system by *S. aureus* biofilm infection was noted in a study by Thurlow et al., who suggested that this lack of response may be related to poor TLR 2/9 recognition of the bacterium when it is encased in the biofilm matrix [51]. TLR signaling is key for eliciting a pro-inflammatory response and immune cell recruitment [52–55], with TLR 2 and 9 playing specific roles in the recognition of *S. aureus* [56–64]. This lack of response is further supported in the current study, which showed several pro-inflammatory markers significantly suppressed at times, including IL-1β, IL-6, IL-12p70, and IFN-γ. Anti-inflammatory markers IL-10 and IL-13 were either suppressed or exhibited minimal change in either DPT or FT burn wounds with infection. These findings are supported by others who have also described anti-inflammatory effects of *S. aureus* [21]. Overall, these results suggest that while neutrophils and macrophages are effectively recruited in response to the burn injury, infection with *S. aureus* leads to an overall repression of cell signaling and host recognition, which may explain the inability to clear or mitigate the *S. aureus* biofilm infection.

The effects of burn wound and infection go beyond just the site of injury. As the wounds progress, the inflammatory signals (including HMGB-1, HYL, and C3) tend to spill over into the circulatory system [65–69]. This is especially true of DAMP signals, which are host derived signals to inform the defense system of a break in homeostasis. Within the confines of this study, infection had minimal effects on HMGB-1, but induced significant reductions in Hyaluronan and C3, as compared to burn-only controls. The mild increases in HMGB-1 in FT infected wounds may be correlated to the minor changes in MPO levels and pathology, where slightly greater inflammation was attributed to faster accumulation of necrotic neutrophils. HMGB-1 is typically released following burn injury, being sourced from macrophages; however, necrotic tissue and accumulation of necrotic neutrophils,

as seen in the FT infected burn wounds, can also result in elevated levels of HMGB-1 [65,66,70]. Reduced levels of HYL in *S. aureus* infected FT burn wounds, particularly at POD 3, correspond and may be related to biofilm formation that was previously discussed. The lack of changes in HYL in the DPT scenario may be related to the observation that FT burn injury significantly increases HYL release at POD 3 due to the extensive injury compared to the DPT injury. HYL is a structural component of the tissue that is typically released following burn wound injury [69,71]. *S. aureus* has been shown to incorporate HYL in its biofilm matrix, along with other polysaccharides, DNA, and proteins, which may explain the decreased HYL levels measured in circulation [61,72,73]. This lack of HYL may also act to reduce TLR2 activation, which would further impede *S. aureus* clearance [69]. While changes in HMGB-1 and HYL are more apparent in FT burn wounds, changes in complement C3 were more significant in DPT burn wounds and may be related to overall *S. aureus* bioburden.

In the case of both DPT and FT infected burn wounds, C3 was reduced by *S. aureus* at all time points for 10^4 and 10^5 inoculums, relative to controls, which suggests that *S. aureus* triggers virulence activity against the immune system prior to biofilm formation. In particular, the significant reduction in C3 for the DPT at PODs 7 and 11 are correlated with the significantly greater abundance of *S. aureus* within the wound, compared to FT at these timepoints. Unlike HYL, the effect of *S. aureus* on C3 inhibition appears to be dependent on the overall population of *S. aureus* within the wound. While complement serves many roles in immunity, it is often associated with opsonization and killing of microorganisms [74,75]. Initial recognition of invading microbes by pattern-recognition proteins begins the complement cascade, which can occur via three pathways: classical, lectin, or alternative [74]. *S. aureus* has been shown to block these cascades through several avenues involving complement C3, including staphylococcal immunoglobin-binding protein (*Sbi*) [76]. *Sbi* forms a complex with C3d and Factor H that leads to futile consumption of C3 into the alternative pathway [21,77]. It should also be noted that *S. aureus* USA300 strain, including TCH1516 strain used in this study, has been found to produce at least two inhibitors of C3 convertase that collectively act to block C3 conversion: staphylococcal complement inhibitor (SCIN) and extracellular adherence protein (EAP) [23,24]. Both SCIN and EAP effectively stop the complement cascade by blocking formation of C3 convertase, which, along with the effects of *Sbi*, leads to decreased phagocytosis of *S. aureus* by neutrophils and macrophages [78–80]. Therefore, while it is likely that C3 is reduced in the serum due to sequestration to the infected wound site, the overall complement cascade may be impaired by *S. aureus* through one or more of these mechanisms and lead to lower systemic levels. Ultimately it is hypothesized that these dynamic changes in complement C3, as well as HMGB-1 and HYL, are dependent on both the degree of injury and *S. aureus* bioburden. Collectively these systemic findings, along with the aforementioned local responses, suggest that this model recapitulates the infectious nature of *S. aureus*, which acts to block overall recognition by the host, thereby attenuating the immune system to clear the infection.

Compared to our previous studies on *P. aeruginosa* biofilm infection within burn wounds, *S. aureus* biofilm infection induces a drastically different host response profile with respect to DAMPs. The more invasive nature and different set of virulence factors excreted from *P. aeruginosa* generates a highly inflamed wound, beyond just the burn injury itself. These infected wounds were noted to have high levels of necrotic neutrophils, elevations in several pro-inflammatory cytokines/chemokines, as well as increased levels of HMGB-1. These results were consistent with clinical *P. aeruginosa* infections, which appear to function in a way to overwhelm the host's immune system through generation of inflammation. *S. aureus* seems to take a more defensive approach by effectively hiding behind enemy lines. As discussed above, *S. aureus* readily forms a biofilm within the burn wound following direct inoculation with as little as 1000 CFUs, providing a more clinically relevant scenario for observing the effects of infection as compared to planktonic interactions of *S. aureus*. Formation of the biofilm allows for *S. aureus* to evade detection

by the host through blockage and/or dysfunction of host communications, including suppression of key cytokine/chemokines and complement C3. While this is in contrast to planktonic studies of *S. aureus*, suppression of inflammatory signals by *S. aureus* in the biofilm state has been seen in other in vivo-based studies, including catheter infections in mice and dermal punch wounds in rabbits [51,81,82]. This suppression of the innate immune system can lead to sequalae of the wound and ultimately cause chronic infection of the burn wound, systemic inflammation, multi-organ failure, sepsis, and/or death [83–86].

While it is believed that this model recapitulates several aspects of *S. aureus* infection within the burn wound, there are still some limitations that should be considered. While rat models have had great utility in the study of burns and infections, it is important to remember that the rat heals by contraction, which is in contrast to humans who heal through re-epithelization and granulation. Additionally, this study was concluded 11 days post-burn, which did not appear to provide enough time for any significant healing within this model based on histopathology assessment (data not shown). Future, studies will look to extend the timeline to at least 21 days post-burn to allow for better investigation of healing and any affects *S. aureus* may have on this process. Despite these limitations, the model still provides a means of observing biofilm infections and can be easily modified to incorporate treatment modalities.

Herein we have applied our previous models of DPT and FT burn wound to *S. aureus* infection. Using a topical application method of *S. aureus* to emulate a real-life exposure scenario, we found that *S. aureus* readily forms biofilms with great consistency, particularly with a 10^5 CFU inoculum, offering a clinically relevant route of infection. This infection resulted in a diminished inflammatory response based on suppression of several cytokines/chemokines and complement C3. These changes in cellular responses and signaling highlight the ability of *S. aureus* biofilms to circumvent the host immune system and provide a clinically relevant model of burn wound infection. Having established a baseline understanding of microbial kinetics and host response within this model of *S. aureus* infection, future studies will focus on more complex infections involving multiple species of microorganisms, as well as testing of novel therapeutics to improve the standard of care in the clinical space and medical readiness for the wounded warrior.

Supplementary Materials: The following are available online at https://www.mdpi.com/article/10.3390/ebj2030009/s1, Figure S1: *S. aureus* and total bioburden within DPT and FT burn wounds with 103 and 104 inoculums; Figure S2: Temporal Changes in *S. aureus* biofilm transcripts; Figure S3: Pathological and MPO changes associated with DPT and FT burn wounds; Figure S4: Temporal changes in local cytokine and chemokine response to *S aureus* infection; Figure S5: DAMP release following DPT and FT burn injury with *S. aureus* infection.

Author Contributions: Conceptualization, A.J.W.J., K.S.B., and K.P.L.; Methodology, A.J.W.J., K.S.B., S.L.R.K., and K.P.L.; Formal Analysis, A.J.W.J. and S.L.R.K.; Investigation, A.J.W.J., K.S.B., S.L.R.K., C.O., and K.P.L.; Resources, K.P.L.; Data Curation, A.J.W.J.; Writing—Original Draft Preparation, A.J.W.J.; Writing—Review and Editing, A.J.W.J., K.S.B., S.L.R.K., and K.P.L.; Visualization, A.J.W.J. and K.S.B.; Supervision, K.P.L.; Project Administration, A.J.W.J., K.S.B., and K.P.L.; Funding Acquisition, K.P.L. All authors have read and agreed to the published version of the manuscript.

Funding: The work was funded in part through the Intramural Program (G_001-2016-USAISR), Combat Casualty Care Research Directorate, US Army Medical Research and Development Command (USAMRDC), and the Naval Medical Research Center's Advanced Medical Development Program (N3239815MHX040). This research was further supported, in part, by the Student Research Participation Program administered by the Oak Ridge Institute for Science and Education through an interagency agreement between the U.S. Department of Energy and USAMRDC.

Institutional Review Board Statement: The study was conducted in compliance with the Animal Welfare Act, the implementing Animal Welfare Regulations, and the principles of the Guide for the Care and Use of Laboratory Animals, National Research Council. The Institutional Animal Care and Use Committee of the U.S. Army Institute of Surgical Research approved all research conducted in this study (DPT study, Protocol# A16-035 approved 31 May 2016; FT study, Protocol# A16-047

approved 15 September 2016). The facility where this research was conducted is fully accredited by the AAALAC.

Data Availability Statement: The data presented in this study are available in the article and accompanying Supplemental Materials.

Acknowledgments: The authors would like to acknowledge Eliza Sebastion, Andrea Fourcadout, and Johnathan Abercrombie for their assistance in bacterial enumeration and histology; and Liwu Qian and Uzziel Pineda for their assistance in animal experiments. The authors would also like to acknowledge the Research Support Division of United States Army Institute of Surgical Research for their assistance in animal care, and particularly COL Brian Smith for his pathological assessment of the tissue.

Conflicts of Interest: The authors declare no conflict of interest. The funders had no role in the design of the study; in the collection, analyses, or interpretation of data; in the writing of the manuscript, or in the decision to publish the results.

References

1. Church, D.; Elsayed, S.; Reid, O.; Winston, B.; Lindsay, R. Burn wound infections. *Clin. Microbiol. Rev.* **2006**, *19*, 403–434. [CrossRef] [PubMed]
2. Kennedy, P.; Brammah, S.; Wills, E. Burns, biofilm and a new appraisal of burn wound sepsis. *Burns* **2010**, *36*, 49–56. [CrossRef]
3. Nunez Lopez, O.; Cambiaso-Daniel, J.; Branski, L.K.; Norbury, W.B.; Herndon, D.N. Predicting and managing sepsis in burn patients: Current perspectives. *Ther. Clin. Risk Manag.* **2017**, *13*, 1107–1117. [CrossRef]
4. Lindberg, R.B.; Moncrief, J.A.; Mason, A.D. Control of experimental and clinical burn wounds sepsis by topical application of sulfamylon compounds. *Ann. N. Y. Acad. Sci.* **1968**, *150*, 950–960. [CrossRef]
5. Chu, C.S.; McManus, A.T.; Pruitt, B.A.; Mason, A.D. Therapeutic effects of silver nylon dressings with weak direct current on Pseudomonas aeruginosa-infected burn wounds. *J. Trauma* **1988**, *28*, 1488–1492. [CrossRef] [PubMed]
6. Kauvar, D.S.; Acheson, E.; Reeder, J.; Roll, K.; Baer, D.G. Comparison of battlefield-expedient topical antimicrobial agents for the prevention of burn wound sepsis in a rat model. *J. Burn Care Rehabil.* **2005**, *26*, 357–361. [CrossRef]
7. McManus, A.T.; McLeod, C.G.; Mason, A.D. Experimental Proteus mirabilis burn surface infection. *Arch. Surg.* **1982**, *117*, 187–191. [CrossRef]
8. Wolf, S.E.; Kauvar, D.S.; Wade, C.E.; Cancio, L.C.; Renz, E.P.; Horvath, E.E.; White, C.E.; Park, M.S.; Wanek, S.; Albrecht, M.A.; et al. Comparison between civilian burns and combat burns from Operation Iraqi Freedom and Operation Enduring Freedom. *Ann. Surg.* **2006**, *243*, 786–792. [CrossRef]
9. World Health Organization. Burns. Available online: https://www.who.int/news-room/fact-sheets/detail/burns (accessed on 28 March 2020).
10. Krishnan, P.; Frew, Q.; Green, A.; Martin, R.; Dziewulski, P. Cause of death and correlation with autopsy findings in burns patients. *Burns* **2013**, *39*, 583–588. [CrossRef]
11. Keen, E.F.; Robinson, B.J.; Hospenthal, D.R.; Aldous, W.K.; Wolf, S.E.; Chung, K.K.; Murray, C.K. Incidence and bacteriology of burn infections at a military burn center. *Burns* **2010**, *36*, 461–468. [CrossRef]
12. Bloemsma, G.C.; Dokter, J.; Boxma, H.; Oen, I.M. Mortality and causes of death in a burn centre. *Burns* **2008**, *34*, 1103–1107. [CrossRef]
13. Sharma, B.R.; Harish, D.; Singh, V.P.; Bangar, S. Septicemia as a cause of death in burns: An autopsy study. *Burns* **2006**, *32*, 545–549. [CrossRef]
14. Diep, B.A.; Sensabaugh, G.F.; Somboonna, N.; Somboona, N.S.; Carleton, H.A.; Perdreau-Remington, F. Widespread skin and soft-tissue infections due to two methicillin-resistant Staphylococcus aureus strains harboring the genes for Panton-Valentine leucocidin. *J. Clin. Microbiol.* **2004**, *42*, 2080–2084. [CrossRef] [PubMed]
15. Olaniyi, R.; Pozzi, C.; Grimaldi, L.; Bagnoli, F. *Staphylococcus aureus*-Associated Skin and Soft Tissue Infections: Anatomical Localization, Epidemiology, Therapy and Potential Prophylaxis. *Curr. Top. Microbiol. Immunol.* **2017**, *409*, 199–227. [CrossRef] [PubMed]
16. Gu, F.F.; Hou, Q.; Yang, H.H.; Zhu, Y.Q.; Guo, X.K.; Ni, Y.X.; Han, L.Z. Characterization of Staphylococcus aureus Isolated from Non-Native Patients with Skin and Soft Tissue Infections in Shanghai. *PLoS ONE* **2015**, *10*, e0123557. [CrossRef]
17. van Belkum, A.; Melles, D.C.; Nouwen, J.; van Leeuwen, W.B.; van Wamel, W.; Vos, M.C.; Wertheim, H.F.; Verbrugh, H.A. Co-evolutionary aspects of human colonisation and infection by Staphylococcus aureus. *Infect. Genet. Evol.* **2009**, *9*, 32–47. [CrossRef]
18. David, M.Z.; Daum, R.S. Community-associated methicillin-resistant Staphylococcus aureus: Epidemiology and clinical consequences of an emerging epidemic. *Clin. Microbiol. Rev.* **2010**, *23*, 616–687. [CrossRef]
19. Hanke, M.L.; Kielian, T. Deciphering mechanisms of staphylococcal biofilm evasion of host immunity. *Front. Cell. Infect. Microbiol.* **2012**, *2*, 62. [CrossRef]

20. Stenzel, W.; Soltek, S.; Sanchez-Ruiz, M.; Akira, S.; Miletic, H.; Schlüter, D.; Deckert, M. Both TLR2 and TLR4 are required for the effective immune response in Staphylococcus aureus-induced experimental murine brain abscess. *Am. J. Pathol.* **2008**, *172*, 132–145. [CrossRef]
21. Thammavongsa, V.; Kim, H.K.; Missiakas, D.; Schneewind, O. Staphylococcal manipulation of host immune responses. *Nat. Rev. Microbiol.* **2015**, *13*, 529–543. [CrossRef]
22. Chavakis, T.; Hussain, M.; Kanse, S.M.; Peters, G.; Bretzel, R.G.; Flock, J.I.; Herrmann, M.; Preissner, K.T. Staphylococcus aureus extracellular adherence protein serves as anti-inflammatory factor by inhibiting the recruitment of host leukocytes. *Nat. Med.* **2002**, *8*, 687–693. [CrossRef]
23. Gaviria-Agudelo, C.; Aroh, C.; Tareen, N.; Wakeland, E.K.; Kim, M.; Copley, L.A. Genomic Heterogeneity of Methicillin Resistant Staphylococcus aureus Associated with Variation in Severity of Illness among Children with Acute Hematogenous Osteomyelitis. *PLoS ONE* **2015**, *10*, e0130415. [CrossRef]
24. Highlander, S.K.; Hultén, K.G.; Qin, X.; Jiang, H.; Yerrapragada, S.; Mason, E.O.; Shang, Y.; Williams, T.M.; Fortunov, R.M.; Liu, Y.; et al. Subtle genetic changes enhance virulence of methicillin resistant and sensitive Staphylococcus aureus. *BMC Microbiol.* **2007**, *7*, 99. [CrossRef]
25. Brandenburg, K.S.; Weaver, A.J.; Qian, L.; You, T.; Chen, P.; Karna, S.L.R.; Fourcaudot, A.B.; Sebastian, E.A.; Abercrombie, J.J.; Pineda, U.; et al. Development of Pseudomonas aeruginosa Biofilms in Partial-Thickness Burn Wounds Using a Sprague-Dawley Rat Model. *J. Burn Care Res.* **2019**, *40*, 44–57. [CrossRef] [PubMed]
26. Brandenburg, K.S.; Weaver, A.J.; Karna, S.L.R.; You, T.; Chen, P.; Stryk, S.V.; Qian, L.; Pineda, U.; Abercrombie, J.J.; Leung, K.P. Formation of Pseudomonas aeruginosa Biofilms in Full-thickness Scald Burn Wounds in Rats. *Sci. Rep.* **2019**, *9*, 13627. [CrossRef] [PubMed]
27. Weaver, A.J., Jr.; Brandenburg, K.S.; Smith, B.W.; Leung, K.P. Comparative Analysis of the Host Response in a Rat Model of Deep-Partial and Full-Thickness Burn Wounds With Pseudomonas aeruginosa Infection. *Front. Cell Infect. Microbiol.* **2019**, *9*, 466. [CrossRef]
28. Gilpin, D.A. Calculation of a new Meeh constant and experimental determination of burn size. *Burns* **1996**, *22*, 607–611. [CrossRef]
29. Leary, S.; Underwood, W.; Anthony, R.; Corey, D.; Grandin, T.; Greenacre, C.; Gwaltney-Brant, S.; McCrackin, M.A.; Meyer, R.; Miller, D.; et al. *AVMA Guidelines for the Euthanasia of Animals*, 2013th ed.; American Veterinary Medical Association: Schaumburg, IL, USA, 2013; pp. 1–102.
30. Sanjar, F.; Weaver, A.J.; Peacock, T.J.; Nguyen, J.Q.; Brandenburg, K.S.; Leung, K.P. Identification of Metagenomics Structure and Function Associated With Temporal Changes in Rat (*Rattus norvegicus*) Skin Microbiome During Health and Cutaneous Burn. *J. Burn Care Res.* **2020**, *41*, 347–358. [CrossRef]
31. Sanjar, F.; Weaver, A.J.; Peacock, T.J.; Nguyen, J.Q.; Brandenburg, K.S.; Leung, K.P. Temporal shifts in the mycobiome structure and network architecture associated with a rat (*Rattus norvegicus*) deep partial-thickness cutaneous burn. *Med. Mycol.* **2020**, *58*, 107–117. [CrossRef]
32. Barbu, E.M.; Mackenzie, C.; Foster, T.J.; Höök, M. SdrC induces staphylococcal biofilm formation through a homophilic interaction. *Mol. Microbiol.* **2014**, *94*, 172–185. [CrossRef]
33. Jenkins, A.; Diep, B.A.; Mai, T.T.; Vo, N.H.; Warrener, P.; Suzich, J.; Stover, C.K.; Sellman, B.R. Differential expression and roles of Staphylococcus aureus virulence determinants during colonization and disease. *MBio* **2015**, *6*, e02272-14. [CrossRef] [PubMed]
34. Gaupp, R.; Schlag, S.; Liebeke, M.; Lalk, M.; Götz, F. Advantage of upregulation of succinate dehydrogenase in Staphylococcus aureus biofilms. *J. Bacteriol.* **2010**, *192*, 2385–2394. [CrossRef] [PubMed]
35. Zhou, C.; Bhinderwala, F.; Lehman, M.K.; Thomas, V.C.; Chaudhari, S.S.; Yamada, K.J.; Foster, K.W.; Powers, R.; Kielian, T.; Fey, P.D. Urease is an essential component of the acid response network of Staphylococcus aureus and is required for a persistent murine kidney infection. *PLoS Pathog.* **2019**, *15*, e1007538. [CrossRef]
36. Archer, N.K.; Mazaitis, M.J.; Costerton, J.W.; Leid, J.G.; Powers, M.E.; Shirtliff, M.E. Staphylococcus aureus biofilms: Properties, regulation, and roles in human disease. *Virulence* **2011**, *2*, 445–459. [CrossRef]
37. Caiazza, N.C.; O'Toole, G.A. Alpha-toxin is required for biofilm formation by Staphylococcus aureus. *J. Bacteriol.* **2003**, *185*, 3214–3217. [CrossRef]
38. Anderson, M.J.; Schaaf, E.; Breshears, L.M.; Wallis, H.W.; Johnson, J.R.; Tkaczyk, C.; Sellman, B.R.; Sun, J.; Peterson, M.L. Alpha-Toxin Contributes to Biofilm Formation among Staphylococcus aureus Wound Isolates. *Toxins* **2018**, *10*, 157. [CrossRef]
39. Scherr, T.D.; Hanke, M.L.; Huang, O.; James, D.B.; Horswill, A.R.; Bayles, K.W.; Fey, P.D.; Torres, V.J.; Kielian, T. Staphylococcus aureus Biofilms Induce Macrophage Dysfunction Through Leukocidin AB and Alpha-Toxin. *MBio* **2015**, *6*, e01021-15. [CrossRef] [PubMed]
40. Yoong, P.; Torres, V.J. The effects of Staphylococcus aureus leukotoxins on the host: Cell lysis and beyond. *Curr. Opin. Microbiol.* **2013**, *16*, 63–69. [CrossRef]
41. Bhattacharya, M.; Berends, E.T.M.; Chan, R.; Schwab, E.; Roy, S.; Sen, C.K.; Torres, V.J.; Wozniak, D.J. biofilms release leukocidins to elicit extracellular trap formation and evade neutrophil-mediated killing. *Proc. Natl. Acad. Sci. USA* **2018**, *115*, 7416–7421. [CrossRef] [PubMed]
42. Paharik, A.E.; Salgado-Pabon, W.; Meyerholz, D.K.; White, M.J.; Schlievert, P.M.; Horswill, A.R. The Spl serine proteases modulate Staphylococcus aureus protein production and virulence in a rabbit model of pneumonia. *mSphere* **2016**, *1*, e00208-16. [CrossRef]

43. Semerad, C.L.; Liu, F.; Gregory, A.D.; Stumpf, K.; Link, D.C. G-CSF is an essential regulator of neutrophil trafficking from the bone marrow to the blood. *Immunity* **2002**, *17*, 413–423. [CrossRef]
44. Gomez-Cambronero, J.; Horn, J.; Paul, C.C.; Baumann, M.A. Granulocyte-macrophage colony-stimulating factor is a chemoattractant cytokine for human neutrophils: Involvement of the ribosomal p70 S6 kinase signaling pathway. *J. Immunol.* **2003**, *171*, 6846–6855. [CrossRef] [PubMed]
45. Arai, K.; Nishida, J.; Hayashida, K.; Hatake, K.; Kitamura, T.; Miyajima, A.; Arai, N.; Yokota, T. Coordinate regulation of immune and inflammatory responses by cytokines. *Rinsho. Byori.* **1990**, *38*, 347–353.
46. Zhang, C.; Li, Y.; Wu, Y.; Wang, L.; Wang, X.; Du, J. Interleukin-6/signal transducer and activator of transcription 3 (STAT3) pathway is essential for macrophage infiltration and myoblast proliferation during muscle regeneration. *J. Biol. Chem.* **2013**, *288*, 1489–1499. [CrossRef]
47. Ushach, I.; Zlotnik, A. Biological role of granulocyte macrophage colony-stimulating factor (GM-CSF) and macrophage colony-stimulating factor (M-CSF) on cells of the myeloid lineage. *J. Leukoc. Biol.* **2016**, *100*, 481–489. [CrossRef]
48. Costerton, J.W.; Stewart, P.S.; Greenberg, E.P. Bacterial biofilms: A common cause of persistent infections. *Science* **1999**, *284*, 1318–1322. [CrossRef]
49. Stewart, P.S.; Costerton, J.W. Antibiotic resistance of bacteria in biofilms. *Lancet* **2001**, *358*, 135–138. [CrossRef]
50. Sharma, D.; Misba, L.; Khan, A.U. Antibiotics versus biofilm: An emerging battleground in microbial communities. *Antimicrob. Resist. Infect. Control* **2019**, *8*, 76. [CrossRef]
51. Thurlow, L.R.; Hanke, M.L.; Fritz, T.; Angle, A.; Aldrich, A.; Williams, S.H.; Engebretsen, I.L.; Bayles, K.W.; Horswill, A.R.; Kielian, T. Staphylococcus aureus biofilms prevent macrophage phagocytosis and attenuate inflammation in vivo. *J. Immunol.* **2011**, *186*, 6585–6596. [CrossRef]
52. Akira, S.; Uematsu, S.; Takeuchi, O. Pathogen recognition and innate immunity. *Cell* **2006**, *124*, 783–801. [CrossRef]
53. Hayashi, F.; Means, T.K.; Luster, A.D. Toll-like receptors stimulate human neutrophil function. *Blood* **2003**, *102*, 2660–2669. [CrossRef] [PubMed]
54. Hertz, C.J.; Kiertscher, S.M.; Godowski, P.J.; Bouis, D.A.; Norgard, M.V.; Roth, M.D.; Modlin, R.L. Microbial lipopeptides stimulate dendritic cell maturation via Toll-like receptor 2. *J. Immunol.* **2001**, *166*, 2444–2450. [CrossRef] [PubMed]
55. Jones, B.W.; Means, T.K.; Heldwein, K.A.; Keen, M.A.; Hill, P.J.; Belisle, J.T.; Fenton, M.J. Different Toll-like receptor agonists induce distinct macrophage responses. *J. Leukoc. Biol.* **2001**, *69*, 1036–1044.
56. Morath, S.; Stadelmaier, A.; Geyer, A.; Schmidt, R.R.; Hartung, T. Synthetic lipoteichoic acid from Staphylococcus aureus is a potent stimulus of cytokine release. *J. Exp. Med.* **2002**, *195*, 1635–1640. [CrossRef]
57. Weber, J.R.; Moreillon, P.; Tuomanen, E.I. Innate sensors for Gram-positive bacteria. *Curr. Opin. Immunol.* **2003**, *15*, 408–415. [CrossRef]
58. Dziarski, R. Recognition of bacterial peptidoglycan by the innate immune system. *Cell Mol. Life Sci.* **2003**, *60*, 1793–1804. [CrossRef]
59. Shimada, T.; Park, B.G.; Wolf, A.J.; Brikos, C.; Goodridge, H.S.; Becker, C.A.; Reyes, C.N.; Miao, E.A.; Aderem, A.; Götz, F.; et al. Staphylococcus aureus evades lysozyme-based peptidoglycan digestion that links phagocytosis, inflammasome activation, and IL-1beta secretion. *Cell Host Microbe* **2010**, *7*, 38–49. [CrossRef]
60. Ip, W.K.; Sokolovska, A.; Charriere, G.M.; Boyer, L.; Dejardin, S.; Cappillino, M.P.; Yantosca, L.M.; Takahashi, K.; Moore, K.J.; Lacy-Hulbert, A.; et al. Phagocytosis and phagosome acidification are required for pathogen processing and MyD88-dependent responses to Staphylococcus aureus. *J. Immunol.* **2010**, *184*, 7071–7081. [CrossRef]
61. Otto, M. Staphylococcal biofilms. *Curr. Top. Microbiol. Immunol.* **2008**, *322*, 207–228. [CrossRef] [PubMed]
62. Mann, E.E.; Rice, K.C.; Boles, B.R.; Endres, J.L.; Ranjit, D.; Chandramohan, L.; Tsang, L.H.; Smeltzer, M.S.; Horswill, A.R.; Bayles, K.W. Modulation of eDNA release and degradation affects Staphylococcus aureus biofilm maturation. *PLoS ONE* **2009**, *4*, e5822. [CrossRef]
63. Bauer, S.; Kirschning, C.J.; Häcker, H.; Redecke, V.; Hausmann, S.; Akira, S.; Wagner, H.; Lipford, G.B. Human TLR9 confers responsiveness to bacterial DNA via species-specific CpG motif recognition. *Proc. Natl. Acad. Sci. USA* **2001**, *98*, 9237–9242. [CrossRef] [PubMed]
64. Hemmi, H.; Takeuchi, O.; Kawai, T.; Kaisho, T.; Sato, S.; Sanjo, H.; Matsumoto, M.; Hoshino, K.; Wagner, H.; Takeda, K.; et al. A Toll-like receptor recognizes bacterial DNA. *Nature* **2000**, *408*, 740–745. [CrossRef]
65. Lantos, J.; Földi, V.; Roth, E.; Wéber, G.; Bogár, L.; Csontos, C. Burn trauma induces early HMGB1 release in patients: Its correlation with cytokines. *Shock* **2010**, *33*, 562–567. [CrossRef] [PubMed]
66. Huang, L.F.; Yao, Y.M.; Dong, N.; Yu, Y.; He, L.X.; Sheng, Z.Y. Association of high mobility group box-1 protein levels with sepsis and outcome of severely burned patients. *Cytokine* **2011**, *53*, 29–34. [CrossRef]
67. Pisetsky, D.S. The role of nuclear macromolecules in innate immunity. *Proc. Am. Thorac. Soc.* **2007**, *4*, 258–262. [CrossRef] [PubMed]
68. Cavassani, K.A.; Ishii, M.; Wen, H.; Schaller, M.A.; Lincoln, P.M.; Lukacs, N.W.; Hogaboam, C.M.; Kunkel, S.L. TLR3 is an endogenous sensor of tissue necrosis during acute inflammatory events. *J. Exp. Med.* **2008**, *205*, 2609–2621. [CrossRef] [PubMed]
69. Scheibner, K.A.; Lutz, M.A.; Boodoo, S.; Fenton, M.J.; Powell, J.D.; Horton, M.R. Hyaluronan fragments act as an endogenous danger signal by engaging TLR2. *J. Immunol.* **2006**, *177*, 1272–1281. [CrossRef]

70. Scaffidi, P.; Misteli, T.; Bianchi, M.E. Release of chromatin protein HMGB1 by necrotic cells triggers inflammation. *Nature* **2002**, *418*, 191–195. [CrossRef]
71. Onarheim, H.; Reed, R.K.; Laurent, T.C. Increased plasma concentrations of hyaluronan after major thermal injury in the rat. *Circ. Shock* **1992**, *37*, 159–163.
72. Ibberson, C.B.; Parlet, C.P.; Kwiecinski, J.; Crosby, H.A.; Meyerholz, D.K.; Horswill, A.R. Hyaluronan Modulation Impacts Staphylococcus aureus Biofilm Infection. *Infect. Immun.* **2016**, *84*, 1917–1929. [CrossRef]
73. Izano, E.A.; Amarante, M.A.; Kher, W.B.; Kaplan, J.B. Differential roles of poly-N-acetylglucosamine surface polysaccharide and extracellular DNA in Staphylococcus aureus and Staphylococcus epidermidis biofilms. *Appl. Environ. Microbiol.* **2008**, *74*, 470–476. [CrossRef]
74. Sinno, H.; Prakash, S. Complements and the wound healing cascade: An updated review. *Plast. Surg. Int.* **2013**, *2013*, 146764. [CrossRef]
75. Gallinaro, R.; Cheadle, W.G.; Applegate, K.; Polk, H.C. The role of the complement system in trauma and infection. *Surg. Gynecol. Obstet.* **1992**, *174*, 435–440.
76. Pruitt, K.D.; Tatusova, T.; Maglott, D.R. NCBI reference sequences (RefSeq): A curated non-redundant sequence database of genomes, transcripts and proteins. *Nucleic Acids Res.* **2007**, *35*, D61–D65. [CrossRef]
77. Burman, J.D.; Leung, E.; Atkins, K.L.; O'Seaghdha, M.N.; Lango, L.; Bernado, P.; Bagby, S.; Svergun, D.I.; Foster, T.J.; Isenman, D.E.; et al. Interaction of human complement with Sbi, a staphylococcal immunoglobulin-binding protein: Indications of a novel mechanism of complement evasion by Staphylococcus aureus. *J. Biol. Chem.* **2008**, *283*, 17579–17593. [CrossRef]
78. Pietrocola, G.; Nobile, G.; Rindi, S.; Speziale, P. Manipulates Innate Immunity through Own and Host-Expressed Proteases. *Front. Cell. Infect. Microbiol.* **2017**, *7*, 166. [CrossRef] [PubMed]
79. Woehl, J.L.; Stapels, D.A.C.; Garcia, B.L.; Ramyar, K.X.; Keightley, A.; Ruyken, M.; Syriga, M.; Sfyroera, G.; Weber, A.B.; Zolkiewski, M.; et al. The extracellular adherence protein from Staphylococcus aureus inhibits the classical and lectin pathways of complement by blocking formation of the C3 proconvertase. *J. Immunol.* **2014**, *193*, 6161–6171. [CrossRef] [PubMed]
80. Rooijakkers, S.H.; Milder, F.J.; Bardoel, B.W.; Ruyken, M.; van Strijp, J.A.; Gros, P. Staphylococcal complement inhibitor: Structure and active sites. *J. Immunol.* **2007**, *179*, 2989–2998. [CrossRef]
81. Snowden, J.N.; Beaver, M.; Beenken, K.; Smeltzer, M.; Horswill, A.R.; Kielian, T. Staphylococcus aureus sarA regulates inflammation and colonization during central nervous system biofilm formation. *PLoS ONE* **2013**, *8*, e84089. [CrossRef] [PubMed]
82. Gurjala, A.N.; Geringer, M.R.; Seth, A.K.; Hong, S.J.; Smeltzer, M.S.; Galiano, R.D.; Leung, K.P.; Mustoe, T.A. Development of a novel, highly quantitative in vivo model for the study of biofilm-impaired cutaneous wound healing. *Wound Repair Regen.* **2011**, *19*, 400–410. [CrossRef] [PubMed]
83. Kallinen, O.; Maisniemi, K.; Böhling, T.; Tukiainen, E.; Koljonen, V. Multiple organ failure as a cause of death in patients with severe burns. *J. Burn Care Res.* **2012**, *33*, 206–211. [CrossRef] [PubMed]
84. Turner, K.H.; Everett, J.; Trivedi, U.; Rumbaugh, K.P.; Whiteley, M. Requirements for Pseudomonas aeruginosa acute burn and chronic surgical wound infection. *PLoS Genet.* **2014**, *10*, e1004518. [CrossRef]
85. Greenhalgh, D.G. Sepsis in the burn patient: A different problem than sepsis in the general population. *Burn. Trauma* **2017**, *5*, 23. [CrossRef] [PubMed]
86. Lin, C.K.; Kazmierczak, B.I. Inflammation: A Double-Edged Sword in the Response to Pseudomonas aeruginosa Infection. *J. Innate Immun.* **2017**, *9*, 250–261. [CrossRef] [PubMed]